CT-MRI Image Fusion-Based Computer-Assisted Navigation Management of Communicative Tumors Involved the Infratemporal-Middle Cranial Fossa

Rong Yang[1,2,3,4] Han Lu[1,2,3,4] Yang Wang[1,2,3,4] Xin Peng[1,2,3,4] Chi Mao[1,2,3,4] Zhiqiang Yi[5] Yuxing Guo[1,2,3,4] Chuanbin Guo[1,2,3,4]

[1] National Clinical Research Center for Oral Diseases, Beijing, P.R. China
[2] National Engineering Laboratory for Digital and Material Technology of Stomatology, Beijing, P.R. China
[3] Beijing Key Laboratory of Digital Stomatology, Beijing, P.R. China
[4] Department of Oral and Maxillofacial Surgery, Peking University School and Hospital of Stomatology, Beijing, P.R. China
[5] Department of Neurosurgery, Peking University First Hospital, Beijing, P.R. China

Address for correspondence Yuxing Guo, MD, National Clinical Research Center for Oral Diseases, 22 Zhongguancun South Avenue, Haidian District, Beijing 100081, PR China (e-mail: gladiater1984@163.com).

J Neurol Surg B Skull Base 2021;82(suppl S3):e321–e329.

Abstract

Objective Computed tomography (CT) and magnetic resonance imaging (MRI) are crucial for preoperative assessment of the three-dimensional (3D) spatial position relationships of tumor, vital vessels, brain tissue, and craniomaxillofacial bones precisely. The value of CT-MRI-based image fusion was explored for the preoperative assessment, virtual planning, and navigation surgery application during the treatment of communicative tumors involved the infratemporal fossa (ITF) and middle cranial fossa.

Methods Eight patients with infratemporal-middle cranial fossa communicative tumors (ICFCTs) were enrolled in this retrospective study. Plain CT, contrast CT, and MRI image data were imported into a workstation for image fusion, which were used for 3D image reconstruction, virtual surgical planning, and intraoperative navigation sequentially. Therapeutic effect was evaluated through the clinical data analysis of ICFCT patients after CT-MRI image fusion-based navigation-guided biopsy or surgery.

Results High-quality CT-MRI image fusion and 3D reconstruction were obtained in all eight cases. Image fusion combined with 3D image reconstruction enhanced the preoperative assessment of ICFCT, and improved the surgical performance via virtual planning. Definite pathological diagnosis was obtained in all four navigation-guided core needle biopsies. Complete removal of the tumor was achieved with one exception among the seven navigation-guided operations. Postoperative cerebrospinal fluid leakage occurred in one patient with recurrent meningioma.

Conclusion CT-MRI image fusion combined with computer-assisted navigation management, optimized the accuracy, safety, and surgical results for core needle biopsy and surgery of ICFCTs.

Keywords
- CT
- MRI
- image fusion
- computer-aided navigation
- infratemporal-middle cranial fossa
- tumor

received
August 13, 2019
accepted after revision
December 24, 2019
published online
February 7, 2020

Georg Thieme Verlag KG,
Rüdigerstraße 14,
70469 Stuttgart, Germany

DOI https://doi.org/10.1055/s-0040-1701603.
ISSN 2193-6331.

Introduction

The infratemporal fossa (ITF) is a complex area that has an anatomically close relation with the middle cranial fossa and the cavernous sinus, and this fossa is located deep to the masseter muscle and ramus of the mandible. Various tumors occurring in this space could involve intracranial cavity through skull base bone invasion,[1,2] which are defined as infratemporal-middle cranial fossa communicative tumors (ICFCTs) in this article. The ITF space is neighbored to parapharyngeal space that contains numerous vital neurovascular structures, such as internal carotid artery (ICA), internal jugular vein (IJV), and IX-XII cranial nerves that communicate the inside and outside of the cranial cavity.[3] Therefore, there are great risks and challenges for diagnosis and treatment of communicative tumors involving ITF and middle cranial fossa.

Injuring surrounding vessels or nerves due to the anatomical complexity of ICFCTs are prone to occur during the operation. The preoperative design using image navigation software is beneficial for analysis of the tumor characteristics, designing of the surgical approach, and predicting the risk of the operation in advance, which could significantly improve the operation safety and reduce its complications. In recent years, the application of computer-aided navigation technology (CANT) has greatly improved the development of surgical treatment for skull base tumor.[4–6] The advantages of CANT in communicative tumors include both the accurate preoperative designing of core needle biopsy or tumor removal, and reliable intraoperative navigation.[7–9] Computed tomography (CT) data was frequently used for computer-aided design and intraoperative navigation. Bony structures and calcified lesion are easily detected by plain CT imaging, and vessels, hemorrhage sites, and blood-supply branches of tumor are susceptive to contrast CT. However, CT is not sensitive for soft tissue detection, even worse in the case of tumor with intracranial tumor extension, or recurrent, interference by artifact (radioactive seeds or titanium clips) tumors.[10] For ICFCTs, magnetic resonance imaging (MRI) has a more well-marked advantage to evaluate the anatomical relationship between the tumor and the dura mater, brain tissue, and the neural foramen.[11–13] Bone invasion can be detected as hypointense rim interruption on MRI.[11] Meanwhile, more information about the tumor and surrounding soft tissue could be afforded by the preoperative MRI diagnosis.

However, various imaging modalities are usually obtained separately, and are not able to display in the same coordinate system.[14] Once various modality imaging data was integrated together, multimodal image fusion generated through layer matching, spatial registration, and geometric transformation, could be achieved on the same spatial coordinates.[15]

In cases of primary, large ITF tumors, identification and segmentation of tumor-sited images in the navigation designing software using single modal image like contrast CT is easy to accomplish.[16] But great difficulty will be met during the delineation of the communicative tumors from the adjacent normal brain tissue using single CT data. Especially in recurrent ICFCTs, the tumor delineation would play an important role for the precise three-dimensional (3D) image reconstruction and following virtual operation designing and navigation-guided biopsy/surgery.[17] The 3D spatial position relationships of tumor, vital vessels, brain tissue, and craniomaxillofacial bones could be judged precisely using CT-MRI fused image on the same spatial coordinate system. The value of CT-MRI-based image fusion was explored for the preoperative assessment, virtual planning, and navigation surgery application during the ICFCT treatment.

Methods

Patients

Eight patients with diagnosis of ICFCT were enrolled in this retrospective study, at Peking University Hospital of Stomatology from February 2011 to September 2018. Informed consent was obtained from all patients and approval was obtained from the institutional review board of the hospital. Plain CT, contrast CT, and MRI were scanned and collected preoperatively to perform the multimodal image fusion and following analysis. Protocol of our clinical work is presented in ►**Fig. 1**.

Image Fusion Procedure

Plain CT, contrast CT, and MRI image data were imported into the iPlan 3.0 software (BrainLab, Germany) to complete image fusion. Plain CT was set as reference image to be integrated with contrast CT and MRI, which were called floating images in this software, respectively. The floating images, contrast CT and MRI, were transformed and resampled with respect to plain CT coordinate. Therefore, they were able to be displayed in the same coordinate system. The process was conducted by automatic image fusion function, and perfected with manual fine-tuning complementally, to confirm the well-built coordinate system based on different modal window check.[18,19] The authors qualitatively estimated the merit of the fusion by assessing the concordance of explicit structures like before.[20] The precision of image fusion was verified by the coincidence of eyeballs and skull bone from the axial, coronal, and sagittal view of MRI and CT images, indicating by the smooth and continuous evolution trending of image edges from CT to MRI images (►**Fig. 2**).[21]

3D image Reconstruction and Virtual Planning

The reconstructed 3D modules were acquired using automatic segmenting technique of the navigation design software (iPlan 3.0, BrainLab). During the analysis of multimodal image fusion data, the cranial-maxilla-facial bones were segmented from plain CT data, ICA and IJV from contrast CT, and a 3D tumor module from the fused CT-MRI images. In the same spatial coordinate system, CT or MRI data could be selected freely as needed to identify the tumor and adjacent soft and bone tissues involved. Then, using the functional module of the navigation design software, the 3D modules could be rotated, perspective transformed, and measured to observe the spatial

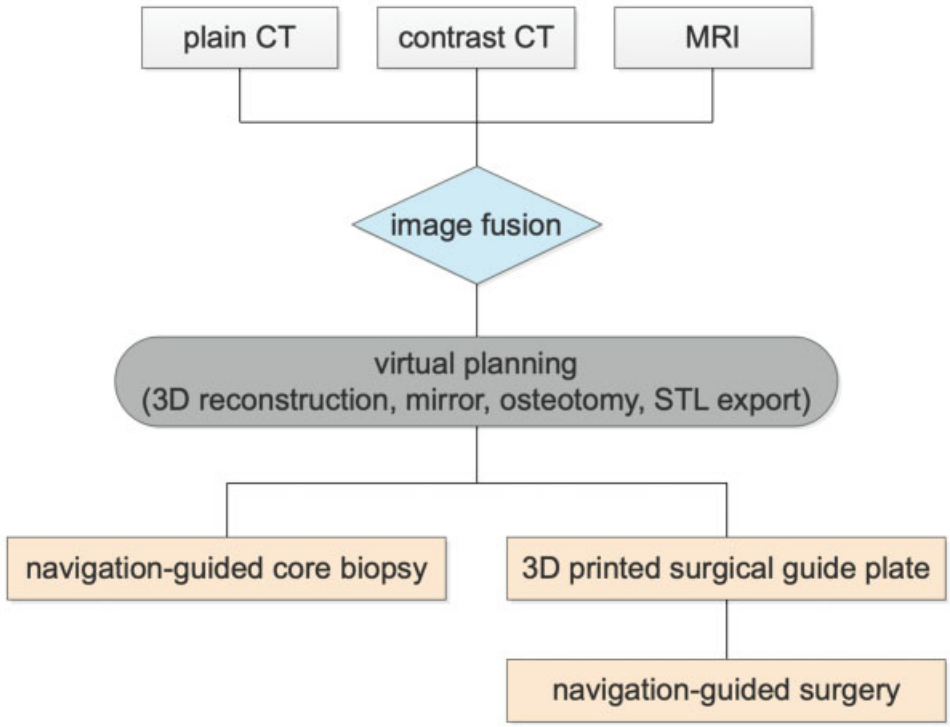

Fig. 1 Protocol of computed tomography (CT)-magnetic resonance imaging (MRI) image fusion-based computer-assisted design and navigation-guided surgery. Plain CT, contrast CT, and MRI data were imported into the design software of navigation system (iPlan 3.0, BrainLab, Germany), and image fusion was performed for each patient preoperatively. The three-dimensional (3D) images of tumor, vital vessels, and craniomaxillofacial bone was reconstructed for preparation of virtual operation design. Operation plan and potential risks were evaluated based on the 3D image. Osteotomy location was designed and 3D model was printed if required. Then, navigation-guided core needle biopsy or tumor-removal surgery was performed under the navigation guidance of the CT-MRI fusion image-based virtual design.

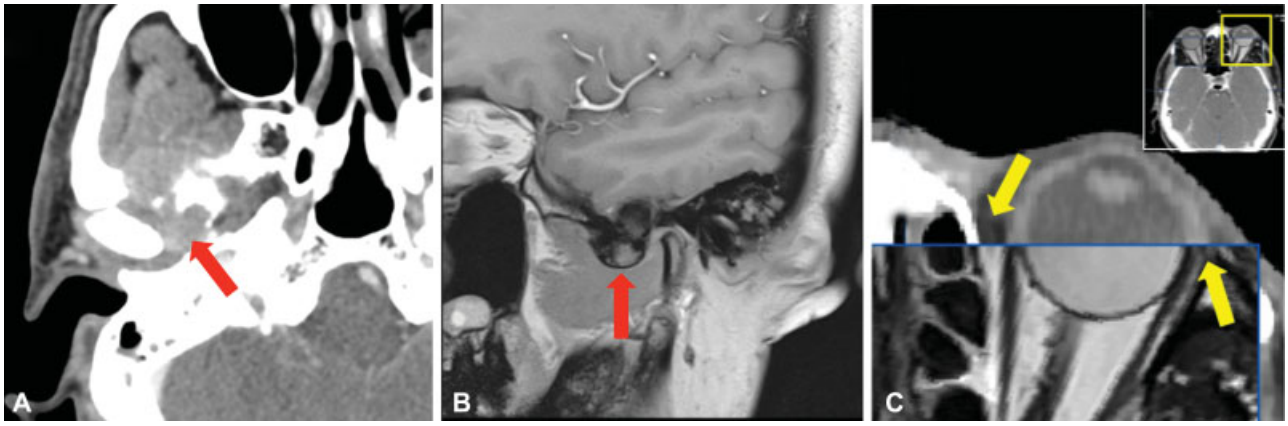

Fig. 2 Demonstration of preoperative image fusion. (**A**) An ill-defined and slightly high-density soft tissue mass with bony destruction (arrow) demonstrated on axial computed tomography (CT) scan. (**B**) A well-defined low signal intensity mass compressing the temporal lobe (arrow) showed on T1-weighted MRI image. (**C**) CT and MRI image fusion was performed. Box shows the coincidence of eyeball contour and adjacent bony boundaries from CT and MRI images, indicating the smooth and continuous evolution trend of image edges from CT (outside of box) to MR images (inside of box).

positional relationship between the tumor and the adjacent vascular/bony structures. The optimal biopsy and/or surgical approaches were simulated and selected afterwards. If needed, ProPlan CMF 3.0 software was used to design the osteotomy line, and standard tessellation language (STL) data could be exported for 3D printed skull-tumor model and surgical guide plates (►**Fig. 3**).

Navigation-Guided Biopsy and Surgery

Navigation-Guided Core Needle Biopsy

The headset was twined on the forehead stably, and the skull reference array with reflective marker spheres was connected with the headset using appropriate adapter. Surface matching technique was used for referencing patients to the navigation system (BrainLab), thus correlation was

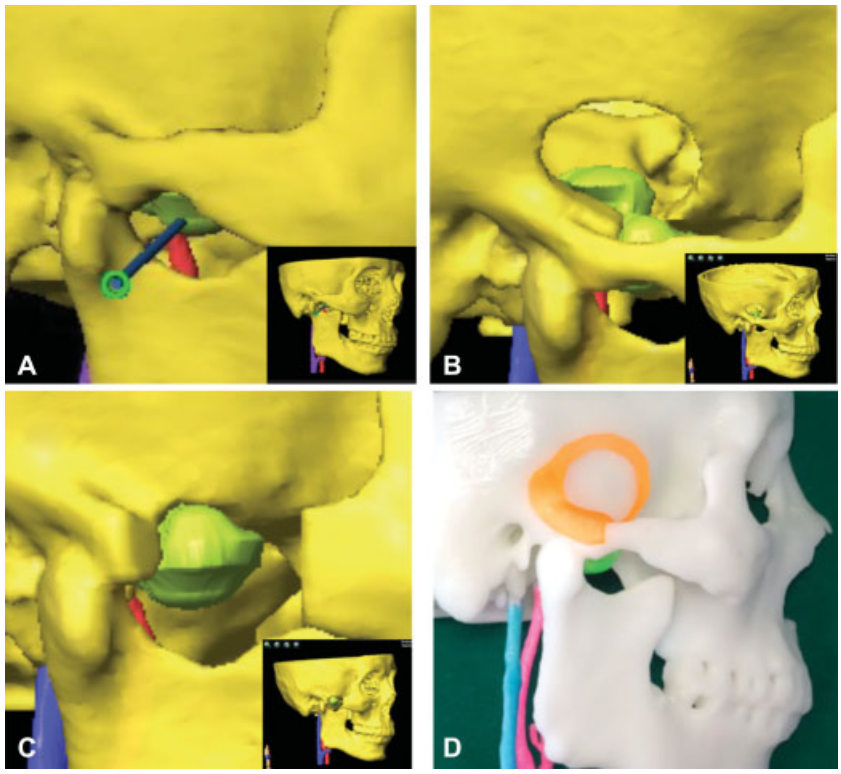

Fig. 3 Three-dimensional (3D) model reconstruction and virtual planning. (**A**) The trajectory path design of navigation-guided core needle biopsy. (**B**) Lateral temporal craniotomy was designed for intracranial part removal of the lesion. (**C**) Zygomatic osteotomy was designed for extracranial part removal of the lesion. (**D**) 3D model with skull, tumor and vessels, and surgical guide plate (orange) were printed. Blue color column indicates the internal jugular vein (IJV), and red color column indicates the internal carotid artery (ICA). The inset shows the 3D image of the overall skull-tumor-vessel model derived from fusion imaging.

established between the face surface data and the preoperative imaging information to obtain real-time interaction. The core needle biopsy instrument (BARD, MG1522) was concatenated to another skull reference array via a designed mental adapter, and integrated into the same coordinate system directed by instrument calibration matrix. The designed puncture site was located with the help of navigation pointer. The core puncture needle passed through the puncture site to arrive at the boundary of the tumor and the normal tissue via the guidance of the navigation monitor. Several repeated biopsies should be performed to get definite diagnosis.[22]

Navigation-Guided Surgery

The skull reference base connected with skull reference array was fixed on the affected side of the parietal bone.[23] Registration procedure was same with above. According to the preoperative design, the tumor was exposed under the guidance of navigation pointer. The tumor was removed under the protection of the vital neurovascular structures, and the guarantee of the operation safety. It was required to use the navigation pointer to confirm the tumor was completely removed without significant structures injury, before completing the operation (►**Fig. 4A, B**).

Image Analysis for Confirmation of Tumor Resection

One week after the operation, postoperative CT image data was imported to the BrainLab software to compare with preoperative image data for confirmation of tumor resection. For patients involving osteotomy, the postoperative and preoperative 3D models of the skull exported from the BrainLab software were compared using Geomagic Studio software to determine whether the osteotomy design from virtual planning was consistent with the actual osteotomy position. The average deviation of the bone structures was calculated automatically (►**Fig. 4C**).

Results

General Clinical Dada

The clinical data of eight patients with ICFCT is shown in ►**Table 1**. There were 4 males and 4 females, with the mean age of 42 (21–61) years. Four of the patients had recurrent tumors and four had primary ones. The clinical symptoms consisted of swelling of auriculotemporal area in five cases, pain and limited mouth opening in four cases, respectively, and one case of temporal skin numbness and hearing loss. Some patients presented with two or more of the above symptoms. After referring to preoperative imaging data, the average maximum diameter of the tumor was approximately 4.34 cm, and the maximum diameter of the skull base bone defect was approximately 1.73 cm. The tumors of four patients originated from the temporomandibular joint, three cases originated from the ITF space, and one case with the intracranial meninges extension into ITF space due to meningioma recurrence.

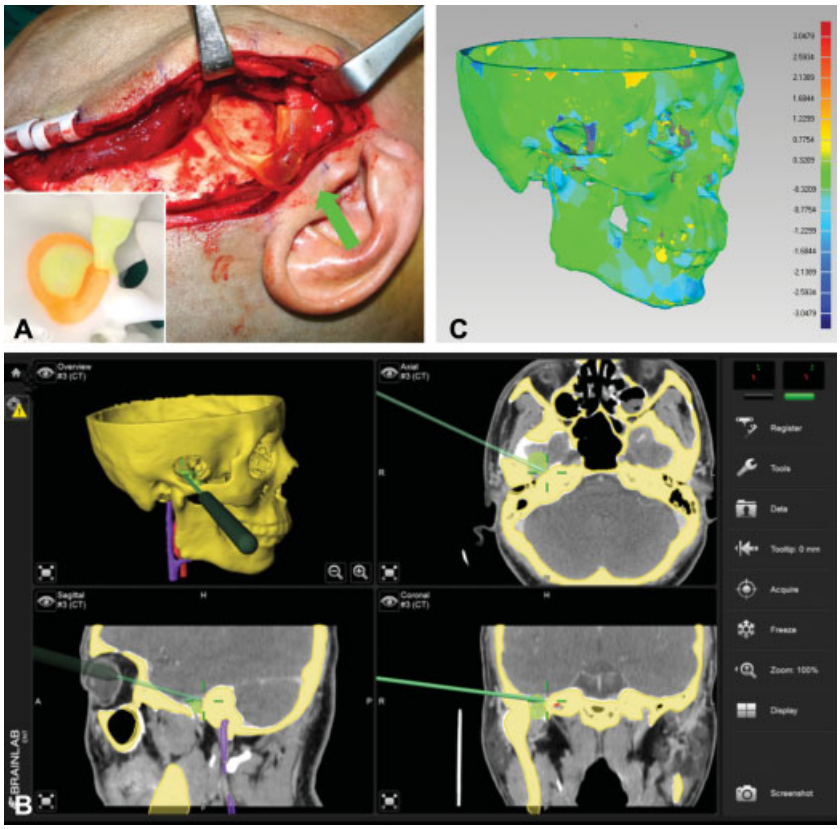

Fig. 4 Navigation-guided surgery implementation to manage infratemporal-middle cranial fossa communicative tumor (ICFCT) and accuracy verification. (**A**) Temporal craniotomy performed precisely using the surgical guide plate (arrow). The inset shows surgical guide plate loaded on stereoscopic model. (**B**) The navigation pointer was used to ascertain the tumor had been completely removed at the end of operation. (**C**) Accuracy verification of the operation by Geomagic Studio software.

Surgery and Pathology Information

The surgical plan designing derived from CT-MRI image fusion technique is easily displayed in 3D mode, and has great value for computer-aided navigation operation, preoperatively. The surgeon acquired the vital information of accurate 3D visual orientation and identification of vital anatomical structures (such as ICA, IJV, and brain tissue) preoperatively and intraoperatively, that would prevent the frequent iatrogenic trauma to the adjacent normal tissues via the real-time navigation.

Navigation-guided core needle biopsies were performed based on multimodal image fusion technique in four primary cases, with definite pathological diagnosis. Navigation-guided surgery was the treatment method for all four recurrent cases and three of the primary cases. Stereotactic intensity radiation therapy was selected for another case, for the impossibility of radical resection due to extensive distribution and ICA involvement. Of the seven cases with navigation-guided surgery, lateral approach (auricular-temporal incision) was used in four cases, inferior approach (lower lip split and mandible swing) in two cases, and maxillary-fronto-temporal approach in one case.[24] The tumors were all completely resected except one that was trigeminal schwannoma that had extension to the cavernous sinus. Pathological diagnosis of all patients is presented in ►**Table 1**.

Postoperative Evaluation, Complication, and Following-Up Investigation

All navigation-guided core biopsies or surgeries were performed successfully. Postoperative image analysis showed that there was no obvious tumor mass left in all cases. The standard deviation from three osteotomy cases was 0.37 ± 0.32, 0.41 ± 0.37, and 0.42 ± 0.33 mm. There was one case of recurrent meningioma with cerebrospinal fluid leakage postoperatively due to the dura mater injury, and was resolved after spinal cerebrospinal fluid drainage. Other patients recovered well without any major complication, and were discharged approximately 1 week after surgery. The follow-up time ranged from 10 to 102 months, and the median follow-up time was 16 months. Image examination was performed periodically (3/6/12 months) postoperation to evaluate whether the tumor recurred. One patient with synovial chondromatosis relapsed after 3 years of first operation, and the pathological diagnosis was synovial sarcoma in repeated surgery. The remaining patients have no signs of recurrence up till now.

Case Report

A 54-year-old female patient came to our unit for consultation, due to the chief complaint of the right facial skin numbness for 6 months (case 1). A soft tissue lump with heterogeneous density in right ITF was displayed on CT

Table 1 General data of the patients

No.	G/A	Chief complaint	Tumor type	Tumor size (cm)	Bone defect (cm)	Original location	Surgical management	Operative approach	Resection degree	Pathological diagnosis	Complication
1	F/54	Skin numbness	P	5.5	2.3	ITF	NGB & NGO	Inferior	Subtotal	Schwannoma	None
2	M/48	Swelling, pain, and limited mouth opening	P	3.4	1.5	TMJ	NGB & NGO	Lateral	Complete	D-TGCT	None
3	M/61	Pain and limited mouth opening	P	2.5	1.1	TMJ	NGB & NGO	Lateral	Complete	D-TGCT & synovial chondromatosis	None
4	M/36	Swelling, pain, and limited mouth opening	P	4.0	1.6	ITF	NGB	–	–	Squamous cell carcinoma	None
5	M/43	Reduced hearing	R	3.7	1.0	ITF	NGO	Inferior	Complete	Neurofibroma	None
6	F/45	Swelling, pain, and limited mouth opening	R	3.6	1.8	TMJ	NGO	Lateral	Complete	D-TGCT	None
7	F/29	Swelling	R	3.0	2.0	TMJ	NGO	Lateral	Complete	Synovial chondromatosis	None
8	F/21	Swelling	R	9.0	2.5	MCF	NGO	Anterior	Complete	Meningioma	CSF

Abbreviations: CSF, cerebrospinal fluid leakage; D-TGCT, diffuse tenosynovial giant cell tumor; F, female; ITF, infratemporal fossa; M, male; MCF, middle cranial fossa; NGB, navigation-guided biopsy; NGO, navigation-guided operation; P, primary; R, recurrent; TMJ, temporomandibular joint.

images. The oval foramen contour and right side of the pituitary fossa was devastated seriously, with incomplete skull base bone. The boundary was not legible between the mass, temporal lobe, and hypophysis. The MRI T2-weighted image showed a 2.9 cm × 3.4 cm × 5.5 cm mass on the right skull base, with clear boundary but uneven internal signal. The intracranial part of the tumor was adjacent to brain temporal lobe, and the dura mater seemed intact. After fusion of CT and MRI images, we evaluated the tumor properties and visually analyzed the spatial position relationship between the tumor and surrounding cranial-maxillofacial bone, ICA/IJV, and brain tissue via reconstructed 3D images on BrainLab software. Meanwhile, the surgical plan was designed and assessed for the potential intraoperative risks. The tumor was removed with the guidance of navigation, using mandibulotomy swing approach. Intracranial part of the tumor was removed under the guidance of navigation system as well as the endoscopic system to ascertain the full degree of tumor resection (►**Fig. 5**). Only flimsy capsule close to the temporal lobe was left for guarantee of the intact dura mater. The pathological diagnosis was manifested to be schwannoma. No obvious tumor mass was found in postoperative CT image (►**Fig. 6**). After 17 months' follow-up, the patient's complaint was significantly relieved, and no explicit signs of recurrence were found on imaging examination.

Discussion

Complex and varied pathological types of communicative tumors could occur between the ITF and the middle cranial fossa. For most communicative tumors, radical resection is the most effective treatment. However, the anatomical structure of the ITF-skull base area is complex and the ITF position locates very deep.[25] The communicative tumors of ITF are not obvious in early stage, and the tumor size becomes much larger when discovered. During the tumor removal procedure, both the protection of the cranial nerves, vital vessels (such as ICA or IJV), and the ascertainment of intact dura mater to avoid cerebrospinal fluid leakage or brain tissue damage need careful identification.[17] Radical resection of the tumor and protection of vital surrounded structures hold equal roles for the optimal ICFCT treatment. Accurate preoperative diagnosis, comprehensive evaluation, and safe operation plan as well as reliable intraoperative navigation are critical to the well-off removal of this type tumor.

For ICFCTs, based on the CT and MRI image fusion, not only the consistency and preliminary diagnosis of the diseased tissue could be judged, but also the integration of their respective advantages could be achieved for the purpose of better computer-aided design. Using computer-aided navigation designing software, 3D reconstruction of craniomaxillofacial bones, ICA, IJV, tumor contour, and brain tissue could be sequentially obtained, for more intuitive and comprehensive evaluation of the relationship between the tumor and surrounding structures by surgeons.[26] Furthermore, fused images provide more understanding about the original ICFCT location.[21] Design of the optimistic biopsy trajectory path, simulation of surgical approach, and osteotomy position that

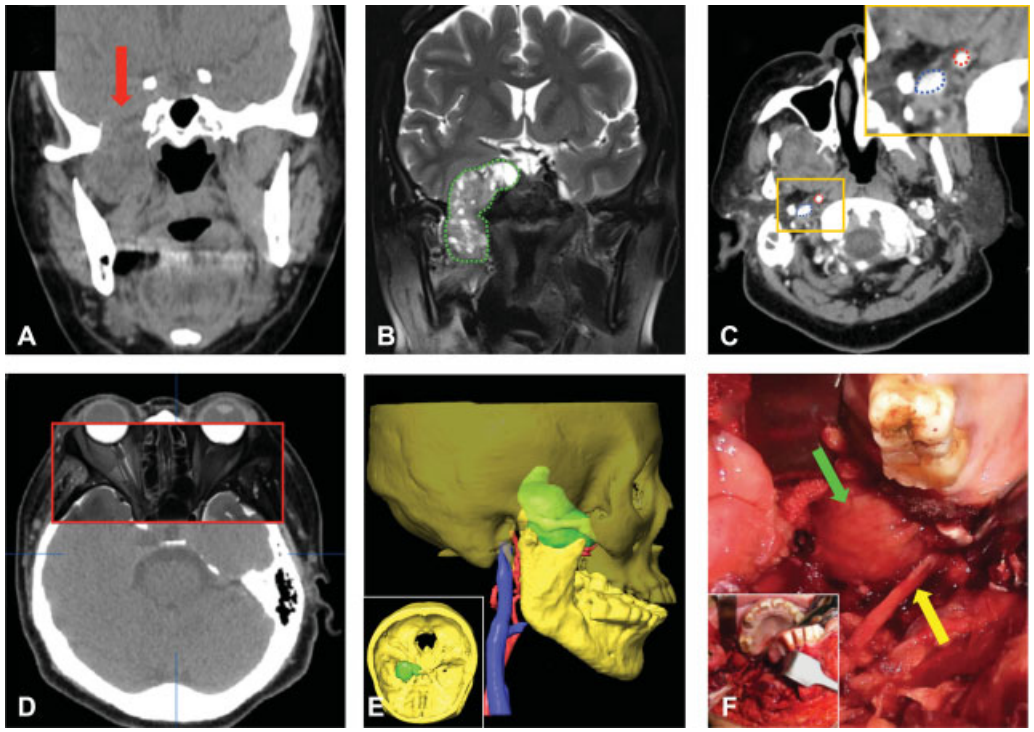

Fig. 5 A 54-year-old female patient complained with the right facial skin numbness for half a year. (**A**) An ill-defined communicative soft tissue tumor bridged the right infratemporal fossa and middle cranial fossa (arrow) showed on plain CT image. (**B**) A heterogeneous high signal mass with clear boundary (dotted line) demonstrated on T2-weighted MRI image. (**C**) Vital vessels such as the internal carotid artery (ICA) (top right dotted line) and internal jugular vein (IJV) (bottom left dotted line) showed clearly on contrast CT scan. The inset shows the boxed region magnified. (**D**) The precision of multimodal image fusion was verified. The contours of eyeball and adjacent bony structures were well coincident between the CT outside of box and MRI images (inside of box). (**E**) Three-dimensional (3D) images of the tumor, craniomaxillofacial bone (60% opacity setting), ICA, and IJV generated from CT-MRI fusion data. The inset shows the superior view of the 3D skull-tumor image. (**F**) The tumor (top arrow) and lingual nerve (bottom arrow) were exposed by mandibular swing approach. The inset shows the overall surgical operation field.

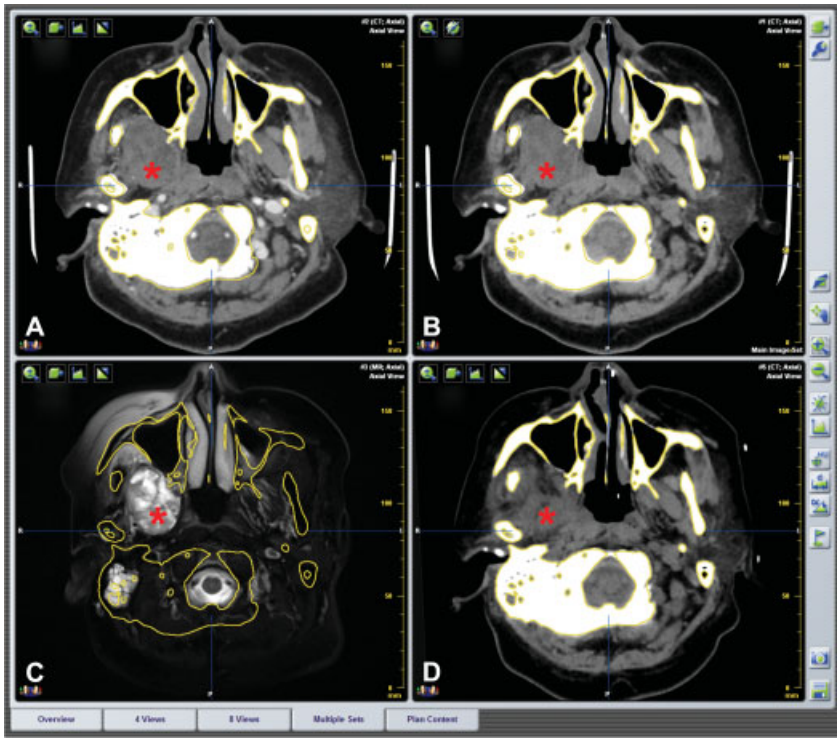

Fig. 6 Fusion images of preoperation and postoperation in the same reference frame. (**A–C**) Preoperative contrast CT, plain CT, and MRI image. Asterisk indicates the tumor area. (**D**) No obvious tumor mass was found in postoperative CT image. The interspace was occupied by muscles and other soft tissues (asterisk).

benefit for tumor removal can also be obtained using the navigation software.[27,28]

To enhance the precision of the operation planning, the accuracy of multimodal image fusion is critical, which depends on many factors, including the quality and resolution of the primary image data, the autofusion algorithm, and the thickness of image scanning slice.[20,29] The BrainLab planning software and its image fusion function has been routinely used in numerous hospitals around the world and assisted physicians in the creation of treatment plans for radiotherapy and neurosurgery.[14,20,30,31] The average image registration accuracy has been evaluated that it is below 1 mm within the intracranial cavity for typical CT-MRI image registrations.[18] The automated fusion function was evaluated by the authors qualitatively. Previous studies have indicated the common practice that experienced surgeons often fine-tune the image fusion if there were any discrepancy with the automated function and the method was proved to have favorable applicability and high accuracy.[18–20,32] It is reported that in the prerequisite of consistent imaging setting and fusion algorithm, the thinner and closer the thickness of imaging scanning slice in different methods, the better is the image fusion accuracy.[30]

Contrast CT and MRI are the first choice for the diagnosis and preoperative evaluation of ICFCT, and function mutually to each other via their respective advantages. At the same time, the incorporated multimodal image fusion combined with reliable navigation technology is beneficial for improving the accuracy and safety of core needle biopsy and surgical treatment for ICFCT.

Funding
This work was supported by the Capital Featured Clinical Application Research Project of Beijing Municipal Science & Technology Commission (Z161100000516043); and the General Program of The National Natural Science Foundation of China (81672664).

Conflict of Interest
None declared.

References

1 Vellutini EAS, Alonso N, Arap SS, et al. Functional reconstruction of temporomandibular joint after resection of pigmented villonodular synovitis with extension to infratemporal fossa and skull base: a case report. Surg J (N Y) 2016;2(03):e78–e82
2 Shin M, Shojima M, Kondo K, et al. Endoscopic endonasal craniofacial surgery for recurrent skull base meningiomas involving the pterygopalatine fossa, the infratemporal fossa, the orbit, and the paranasal sinus. World Neurosurg 2018;112:e302–e312
3 Yacoub A, Anschuetz L, Schneider D, Wimmer W, Caversaccio M. Minimally invasive lateral endoscopic multiport approach to the infratemporal fossa: a cadaveric study. World Neurosurg 2018; 112:e489–e496
4 Guo YX, Sun ZP, Liu XJ, Bhandari K, Guo CB. Surgical safety distances in the infratemporal fossa: three-dimensional measurement study. Int J Oral Maxillofac Surg 2015;44(05):555–561
5 Hayashi N, Kurimoto M, Hirashima Y, et al. Efficacy of navigation in skull base surgery using composite computer graphics of magnetic resonance and computed tomography images. Neurol Med Chir (Tokyo) 2001;41(07):335–339
6 Bell RB. Computer planning and intraoperative navigation in cranio-maxillofacial surgery. Oral Maxillofac Surg Clin North Am 2010;22(01):135–156
7 Abi-Jaoudeh N, Kruecker J, Kadoury S, et al. Multimodality image fusion-guided procedures: technique, accuracy, and applications. Cardiovasc Intervent Radiol 2012;35(05):986–998
8 Wei B, Sun G, Hu Q, Tang E. The safety and accuracy of surgical navigation technology in the treatment of lesions involving the skull base. J Craniofac Surg 2017;28(06):1431–1434
9 Terpolilli NA, Rachinger W, Kunz M, et al. Orbit-associated tumors: navigation and control of resection using intraoperative computed tomography. J Neurosurg 2016;124(05):1319–1327
10 Nemec SF, Donat MA, Mehrain S, et al. CT-MR image data fusion for computer assisted navigated neurosurgery of temporal bone tumors. Eur J Radiol 2007;62(02):192–198
11 Choi HY, Yoon DY, Kim ES, et al. Diagnostic performance of CT, MRI, and their combined use for the assessment of the direct cranial or intracranial extension of malignant head and neck tumors. Acta Radiol 2019;60(03):301–307
12 Zhang SX, Han PH, Zhang GQ, et al. Comparison of SPECT/CT, MRI and CT in diagnosis of skull base bone invasion in nasopharyngeal carcinoma. Biomed Mater Eng 2014;24(01):1117–1124
13 Le Y, Chen Y, Zhou F, Liu G, Huang Z, Chen Y. Comparative diagnostic value of 18F-fluoride PET-CT versus MRI for skull-base bone invasion in nasopharyngeal carcinoma. Nucl Med Commun 2016;37(10):1062–1068
14 Kraeima J, Dorgelo B, Gulbitti HA, et al. Multi-modality 3D mandibular resection planning in head and neck cancer using CT and MRI data fusion: a clinical series. Oral Oncol 2018; 81:22–28
15 Inoue HK, Nakajima A, Sato H, Noda SE, Saitoh J, Suzuki Y. Image fusion for radiosurgery, neurosurgery and hypofractionated radiotherapy. Cureus 2015;7(03):e252
16 Dai J, Wang X, Dong Y, Yu H, Yang D, Shen G. Two- and three-dimensional models for the visualization of jaw tumors based on CT-MRI image fusion. J Craniofac Surg 2012;23(02):502–508
17 Chiu AG, Palmer JN, Cohen N. Use of image-guided computed tomography-magnetic resonance fusion for complex endoscopic sinus and skull base surgery. Laryngoscope 2005;115(04): 753–755
18 Grosu AL, Lachner R, Wiedenmann N, et al. Validation of a method for automatic image fusion (BrainLAB System) of CT data and 11C-methionine-PET data for stereotactic radiotherapy using a LINAC: first clinical experience. Int J Radiat Oncol Biol Phys 2003;56(05): 1450–1463
19 Bamba Y, Nonaka M, Nakajima S, Yamasaki M. Three-dimensional reconstructed computed tomography-magnetic resonance fusion image-based preoperative planning for surgical procedures for spinal lipoma or tethered spinal cord after myelomeningocele repair. Neurol Med Chir (Tokyo) 2011;51(05):397–402
20 Thani NB, Bala A, Swann GB, Lind CR. Accuracy of postoperative computed tomography and magnetic resonance image fusion for assessing deep brain stimulation electrodes. Neurosurgery 2011; 69(01):207–214
21 Leong JL, Batra PS, Citardi MJ. CT-MR image fusion for the management of skull base lesions. Otolaryngol Head Neck Surg 2006;134(05):868–876
22 Guo YX, Peng X, Liu XJ, Zhang L, Yu GY, Guo CB. Application of computer-aided design and navigation technology in skull base and infratemporal fossa tumor surgery [in Chinese]. Zhonghua Kou Qiang Yi Xue Za Zhi 2013;48(11):645–647
23 Guo R, Guo YX, Feng Z, Guo CB. Application of a computer-aided navigation technique in surgery for recurrent malignant infratemporal fossa tumors. J Craniofac Surg 2015;26(02):e126–e132
24 Guo Y, Guo C. Maxillary-fronto-temporal approach for removal of recurrent malignant infratemporal fossa tumors:

anatomical and clinical study. J Craniomaxillofac Surg 2014;42 (03):206–212
25 Nonaka Y, Fukushima T, Watanabe K, Sakai J, Friedman AH, Zomorodi AR. Middle infratemporal fossa less invasive approach for radical resection of parapharyngeal tumors: surgical microanatomy and clinical application. Neurosurg Rev 2016;39(01): 87–96
26 Xu TF, Duan WC, Lu T, Chen L. Application of three-dimensional reconstruction technique based on CT-MRI fusion in skull base surgery [in Chinese]. Zhonghua Er Bi Yan Hou Tou Jing Wai Ke Za Zhi 2012;47(05):373–378
27 Yu HB, Li B, Zhang L, Shen SG, Wang XD. Computer-assisted surgical planning and intraoperative navigation in the treatment of condylar osteochondroma. Int J Oral Maxillofac Surg 2015;44 (01):113–118
28 Azarmehr I, Stokbro K, Bell RB, Thygesen T. Surgical navigation: a systematic review of indications, treatments, and outcomes in oral and maxillofacial surgery. J Oral Maxillofac Surg 2017;75 (09):1987–2005
29 Nemec SF, Peloschek P, Schmook MT, et al. CT-MR image data fusion for computer-assisted navigated surgery of orbital tumors. Eur J Radiol 2010;73(02):224–229
30 Sato M, Tateishi K, Murata H, et al. Three-dimensional multimodality fusion imaging as an educational and planning tool for deep-seated meningiomas. Br J Neurosurg 2018;32(05):509–515
31 Han Z, Bondeson JC, Lewis JH, et al. Evaluation of initial setup accuracy and intrafraction motion for spine stereotactic body radiation therapy using stereotactic body frames. Pract Radiat Oncol 2016;6(01):e17–e24
32 Yu Y, Zhang WB, Liu XJ, et al. Three-dimensional image fusion of (18)F-fluorodeoxyglucose-positron emission tomography/computed tomography and contrast-enhanced computed tomography for computer-assisted planning of maxillectomy of recurrent maxillary squamous cell carcinoma and defect reconstruction. J Oral Maxillofac Surg 2017;75:1301, e1301–1301, e1315
33 Sekhar LN, Schramm VL Jr, Jones NF. Subtemporal-preauricular infratemporal fossa approach to large lateral and posterior cranial base neoplasms. J Neurosurg 1987;67(04):488–499